Aus der Augenklinik der Medizinischen Fakultät der Universität Rostock:

# PHENOTYPE CHARACTERIZATION IN MACULAR DYSTROPHIES: THE ROLE OF MULTIFOCAL ELECTRORETINOGRAPHY AND HIGH-RESOLUTION OPTICAL COHERENCE TOMOGRAPHY

Habilitationsschrift

zur

Erlangung des akademischen Grades

doctor medicinae habilitata (Dr. med. habil.)

der Medizinischen Fakultät der Universität Rostock

vorgelegt von: Dr. med. Christina Gerth,

geb. am 22.12.1969 in Altenburg

wohnhaft in: Rostock

Rostock, den 30.3.2009

urn:nbn:de:gbv:28-diss2010-0018-7

**Gutachter:**

Prof. Dr. M. Bach,

Augenklinik der Universität Freiburg

Prof. Dr. med. R.Guthoff,
Augenklinik der Universität Rostock

Prof. Dr. med. K. Rüther,

Humboldt Universität zu Berlin, Augenklinik, Charité Campus Virchow-Klinikum

Verteidigung am: 30.11.2009

**TABLE OF CONTENT**

# 1. INTRODUCTION

Retinal dystrophies have a high impact on a patient's life: reduced central and or peripheral vision, night blindness, photophobia and/ or even blindness can occur depending on diseased retinal cells and retinal area. The macula area, only or primarily, is affected in a subset of retinal dystrophies. Stargardt macular dystrophy[1] (STGD1) is one of the most common hereditary macular dystrophies[2], whereas age-related macular degeneration (AMD) is the leading cause of 'elderly' blindness in developed countries.[3]

Phenotype characterization is essential to identify the type of retinal dystrophy for patient information and counseling. Phenotype identification will guide molecular-genetic investigations based on specific features of the underlying retinal changes. The next aim is retinal morphology and function quantification over time to understand the longitudinal natural disease course. Of major interest are early disease stages. In particular children need special attention and technical setups for collecting data. Our focus was to develop a method, which would allow imaging infants and children for retinal morphology analysis. Once the disease causing mutation is identified, genotype-phenotype correlation is the next step in studying retinal dystrophies. New promising trials in retinal dystrophies are arising. For this, objective outcome measures are a necessity for successful therapies.

Retinal function and morphology are the two foundations of phenotypic characterization. Retinal function can be measured objectively by electroretinography. The multifocal electroretinogram (mfERG) allows a detailed mapping of retinal and macular function. First, no detailed knowledge of age-related changes in mfERG responses and their origin was available. Investigations into the natural aging process allowed longitudinal studies in different age groups to be made.

Studies of in-vivo retinal morphology were limited by technical properties. Optical coherence tomography (OCT)[4], a fairly new in-vivo imaging technique in ophthalmology permits visualizing of retinal morphology in cross-sectional scans [reviewed in[5]] and, with the use of more advanced reconstructing programs in 3-D view similarly to a CT scan.[6] We used this technique to quantify macular dystrophies together with retinal function in a wide range of retinal and macular dystrophies.

This work summarizes research performed during my residency at the University of Regensburg, the research fellowships and visits at the Vision Science and Advanced Retinal Imaging Laboratory (VSRI) at the Department of Ophthalmology and Vision Science, University of California, Davis, USA and the Department of Ophthalmology and Vision Sciences, The Hospital for Sick Children in Toronto, Canada.

## 2. METHODS

### 2.1. Multifocal electroretinography (mfERG)

#### 2.1.1. Basic principles

Electroretinography (ERG) using different stimulus and background light intensities allows measuring retinal activity. It is a standard measure in vision science to quantify retinal cell function.[7] ERGs can be recorded from the entire retina by using a flash stimulus (fullfield ERG) or from areas with a focal stimulus. The multifocal technique introduced by Sutter and Tran[8] permits recordings of multiple, spatially localized ERGs and therefore, mapping of macular function. Hood et al.[9] showed that the first-order kernel response in photopic mfERGs is generated from the cone photoreceptor cells and the ON- and OFF bipolar cells. Localized abnormal retinal responses, which are undetected by the fullfield ERG can now be identified and mapped using the mfERG. 103 individual hexagonal areas within a retinal area of 15-25 degrees in radius (about the area of the posterior pole containing most morphological changes in macular dystrophies) can be tested and mapped. This technique is therefore useful and efficient, in detecting abnormal responses in the early stage of disease, in mapping abnormal responses in the cone-driven pathways and in monitoring disease progression.

#### 2.1.2. MfERG recording

MfERG responses were recorded according to the recommended ISCEV guidelines for basic mfERG.[10] We used a 103 hexagon stimulation (Fig.1) displayed on a VERIS$^{TM}$ stimulus-refractor unit (frame rate 75 Hz) or on a large screen[11] and a standard m-sequence length with m=14. Signals were sampled at 1200 Hz (i.e. 0.83 ms between samples). Stimulus luminance ranged between 135 and 700 cd $\cdot$ m$^{-2}$ (white) and <1 cd $\cdot$ m$^{-2}$ cd (black). Data were acquired at a gain of $10^5$ over a frequency range of 10-300 Hz. All mfERGs were recorded monocular with dilated pupils using a bipolar Burian-Allen electrode and an electrode placed on the forehead as a ground electrode. Subjects were asked to focus on a fixation target displayed within the stimulus array, or, in case of reduced visual acuity, in the middle of an enlarged cross.

First-order kernel mfERG responses were analyzed for response density (density scale average obtained from the first negative trough to the first positive peak) and implicit times (first and second negative through and first positive peak). (Fig. 1)

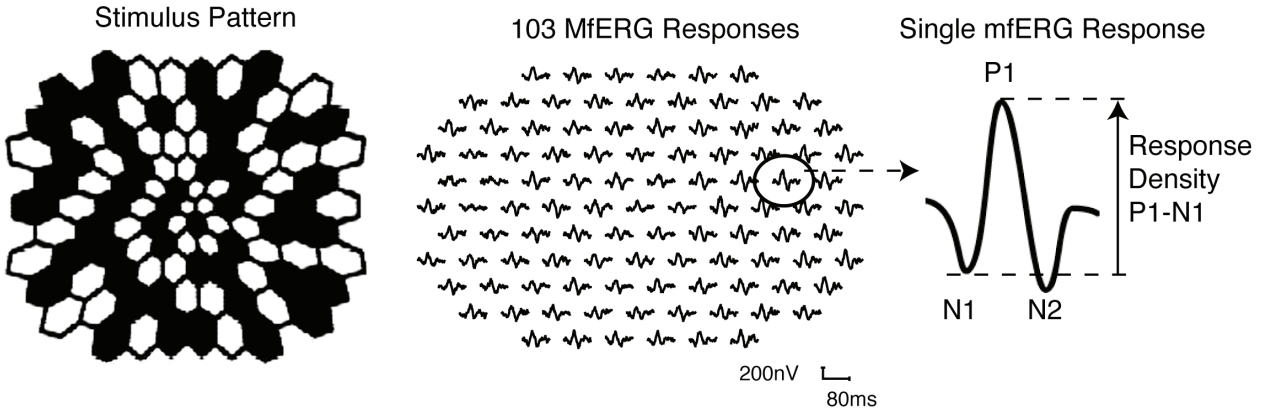


*Figure 1: MfERG stimulus pattern of 103 hexagons (left) and resulting retinal responses in a control subject shown (middle). Single MfERG responses are analyzed for response density P1-N1 and implicit times N1, P1 and N2 (right).*

There are different options for response analysis. Each of the single mfERG response can be analyzed separately or grouped into areas or concentric rings. The latter way of analysis is advantageous for recordings with small signals or low signal-to-noise ratio (SNR) and for calculating ratios. The disadvantage of grouping is the loss of the localized response characteristic, the strength of the mfERG. We applied the concentric ring analysis in order to visualize age-related changes in a normative data group topographically.[12, 13] We also analyzed mfERG data from patients with Stargardt Macular Dystrophy in the same way to overcome the problems of small signals from diseased retinal areas.[11] Further analysis of patient data was performed for each retinal area stimulated after carefully controlling for SNR.[14-16] A localized analysis allowed correlations with morphological retinal changes.

Patients with severe or advanced retinal dystrophies show only small retinal responses when tested with the mfERG. (Ref. 6)[16] Data analysis need to consider careful exclusion of noise and artifacts within the signal. (Ref. 7)[17]

### 2.1.3. Age-related response changes

The knowledge of normative data and its age-related change is fundamental for interpretation of patient data. Histological data revealed a cone photoreceptor density loss with age.[18] Fullfield ERG responses showed a linear change in amplitude and latency.[19-21] We therefore hypothesized that retinal responses from the central retina show similar changes with age as indicated by psychophysical experiments.[22] We tested 81 subjects ages 9 to 80 years to investigate the age-

related changes depending on retinal topography. (Ref. 2)[12] All subjects were free of any retinal or optical media changes.

An example of mfERG responses of a 16- and a 72-year old control subject is shown in Fig. 2.

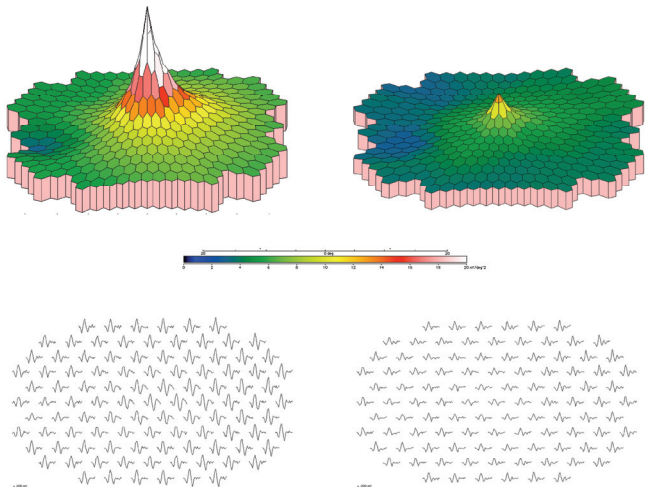

*Figure 2: Central retinal mfERG responses of a 16- (left panel) and a 72-year old subject (right panel) demonstrate an obvious decline with age. Trace arrays (bottom) with corresponding response density plots (top row) show a larger reduction in the central than in the peripheral responses.*

We found a significant decline in retinal responses with age for all retinal areas with the steepest slope in the central response compared with extrafoveal responses. (Fig. 3) Implicit time P1 changed with age but there was no difference with retinal topography.

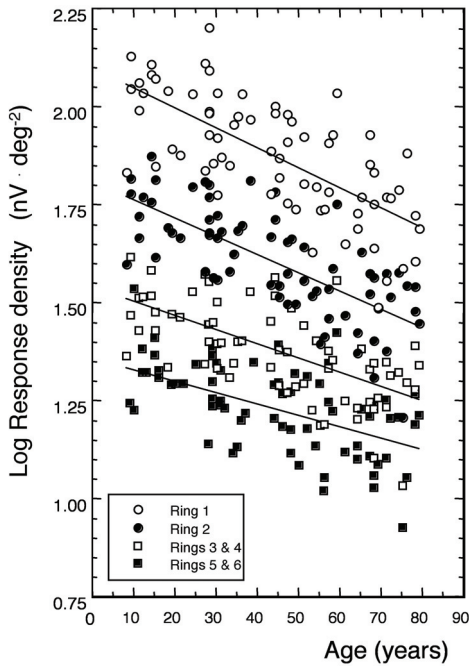


*Figure 3: Log response density is plotted as a function of age for different concentric retinal areas stimulated. Least-squares linear regression lines are shown for each data set.*

Are the age-related changes in retinal responses different for different luminances? All subjects were tested twice, with 200 cd · $m^{-2}$ and 700 cd · $m^{-2}$ white stimuli. The rate of change with age was not significantly different for the two testing conditions indicating a stable visual system for the luminances tested.

A previous publication investigating the aging effect on retinal responses claimed it to be caused by optical factors.[23] We hypothesized that some but not all aging effects are caused by optical factors, but an important part are caused by neural factors in the visual system.

We simulated the effect of increasing scatter and loss of contrast and retinal illuminance due to optical changes with age. After subtracting those effects from the mfERG response, there was still a change, which can be attributed to senescent changes within the cone pathways.

These results have an important impact on the analysis of mfERG data. Studies performed in a patient cohort of different ages need to compare the data with a detailed normative database obtained on the same recording system and under the same recording conditions. Longitudinal studies of elderly patients, who receive cataract surgery during the observation time, need to take the changed optical media into account for data interpretation.

The first-order kernel mfERG response is far more complex than a fullfield ERG response. Lateral and temporal retinal interactions occur because of the fast stimulation of multiple retinal areas. The mfERG response contains the response to the stimulus (isolated flash response) and induced components from previous and following flash responses (backward and forward interaction).[24] We investigated the effect on mfERG responses for different interactions to get insight in the origin of retinal response aging within the cone pathways. (Ref. 3)[13] Our detailed analysis of mfERG response components revealed a senescent change in the isolated flash response more than in consecutive flash interactions. Optical and neural factors are responsible for this aging decline, with the latter over weighting the first. We then repeated the analysis for the same retinal area that we had tested with psychophysical measures.[25] Both responses, the isolated flash response elicited by the mfERG and the impulse response function using a double-pulse method, indicated a response amplitude decline and a small but significant increase in implicit time. Thus, the aging effect occurs early in the visual system, the retina. Adaptive mechanism, such as gain control within the visual system might compensate for some but not all of the aging effect in the retinal response.[26]

The results provide the basis for further studies in patients with macular dystrophies.

## 2.2. Optical coherence tomography (OCT)

### 2.2.1. Basic principles

The underlying principle of the OCT is to image biological tissue trough the reflection of light. It is in contrast to the ultrasound technique a non-contact application. The application of light allows a much higher resolution than ultrasound. Light of 200-600 nm and above 1000 nm wavelength is not used because of tissue absorption by hemoglobin and water, respectively. A light beam, mostly around 800 nm wavelength, is swept across biological tissue. The reflected light is collected and its time-delay measured in comparison with a sample reflection by a Michelson interferometer.[4] The axial resolution is depending on the spectral bandwidth and therefore limited by the development of superluminescent diode. The lateral (transverse) resolution is determined by the optical system to minimize the spot size.

Two main OCT technologies are available: the Time and Fourier domain OCT.

In Time domain OCT, the OCT signal is measured as a function of reference mirror position. In Fourier-domain (FD) OCT the position of the reference mirror is stationary with resulting higher acquisition speed. Signals in FD-OCT systems are detected in Fourier space and then inverse Fourier transformed.

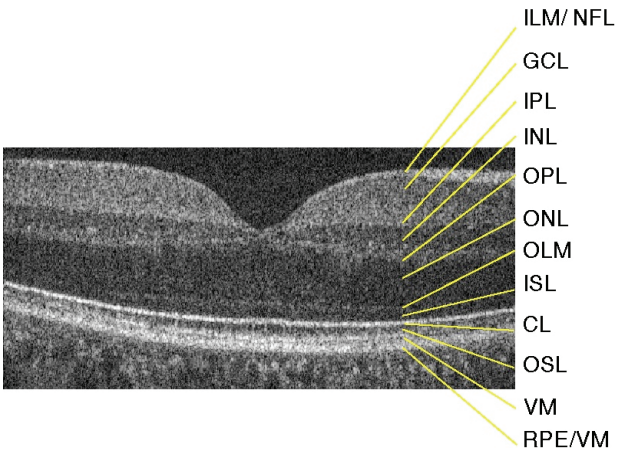


*Figure 4: 6 mm horizontal FD-OCT scan through the macula of a control subject. Retinal layers: CL, connecting cilia; GCL, ganglion cell layer; ILM/ NFL, internal limiting membrane/ nerve fiber layer; INL, inner nuclear layer; IPL, inner plexiform layer; ISL, inner segment layer; OLM, outer limiting membrane; ONL, outer nuclear layer; OPL, outer plexiform layer; OSL, outer segment layer; RPE/BM, retinal pigment epithelium/Bruch's membrane; VM, Verhoeff's membrane.*

The OCT system developed and built at the VSRI is a high-speed FD-OCT[27] with a fast acquisition time (1000 A-scans/ frame, 9 frames/sec) and high resolution (axial 4.5 μm) allowing high-quality imaging in a short time.
This system with high-resolution properties provides image acquisition at near histological level. Single retinal layers are visible and distinguishable in each of the scans as demonstrated in Fig. 4.

### 2.2.2. Mode of application

In the conventional setup patients sit with their head on a chin rest as for a slit-lamp examination. The available table-mounted OCT systems and the necessity of a chin rest do not easily permit scanning in infants and children. We were able to overcome this in collaboration between the VSRI at UC Davis and the Department of Ophthalmology and Vision Sciences at the Hospital of Sick Children in Toronto. (Ref. 14)[28] We used a handheld probe in 2 ways. Children old enough to sit or stand with their head positioned quietly on a chin rest were imaged with the probe mounted on a slit-lamp stand. We used the probe like a hand-held camera for imaging under sedation and in children, who were too young or restless be examined on the mounted system. (Fig. 5)

*Figure 5: The hand-held scanner mounted on a slit-lamp post (left panel) was used for older children. Younger children, not able to sit quietly, and children under sedation (right panel) were imaged in a supine position with the scanner in hand-held mode.*[28]

We were able to image successfully all 30 children included in the study with or without retinal pathology who ranged in age from 7 months to 9.9 years. All children tolerated the procedure well. Children as young as 3 years were able to hold still for image acquisition. We dilated the pupils in most of the children. Some, who did not want eye drops, were cooperative enough to be imaged successfully with undilated pupils.

Slower acquisition systems do not permit imaging subjects with unstable fixation or children. The fast acquisition time of the FD-OCT system used permitted a high image quality despite the sometimes limited attention range. We were able to image children or patients with severely reduced vision and/ or nystagmus.[29-31] Retinal layer resolution in children was similar to that obtained in adults.

Identification of retinal pathology in children imaged was important to exclude non-organic vision loss, quantify abnormal retina layers and complement the clinical diagnosis. In one 7-year old girl, who lost vision due to Leber Congenital Amaurosis, caused by a mutation in the *RPE65* gene, we identified well-preserved inner retinal layers despite nystagmus and unsteady fixation. Outer and inner segment layer were not distinguishable in her macula. This knowledge will be important in upcoming treatment trials to monitor outcome.

### 2.2.3. Data analysis

Retinal layer thickness and morphological changes can be measured and qualitatively analyzed. Raw OCT data undergoes post-processing and reconstruction to obtain en-face fundus OCT scans. A series of B scans is acquired over a retinal area. The system we used was set to obtain 1000 A scans for one B scan. A series of 100 B scans were acquired over an area of 6 x 6 x 2 mm volume of retina. An example of a B scan series is shown in Figure 6. This volumetric scan series can be used for OCT fundus reconstruction and spatial identification of retinal layers abnormalities. (Fig. 7)

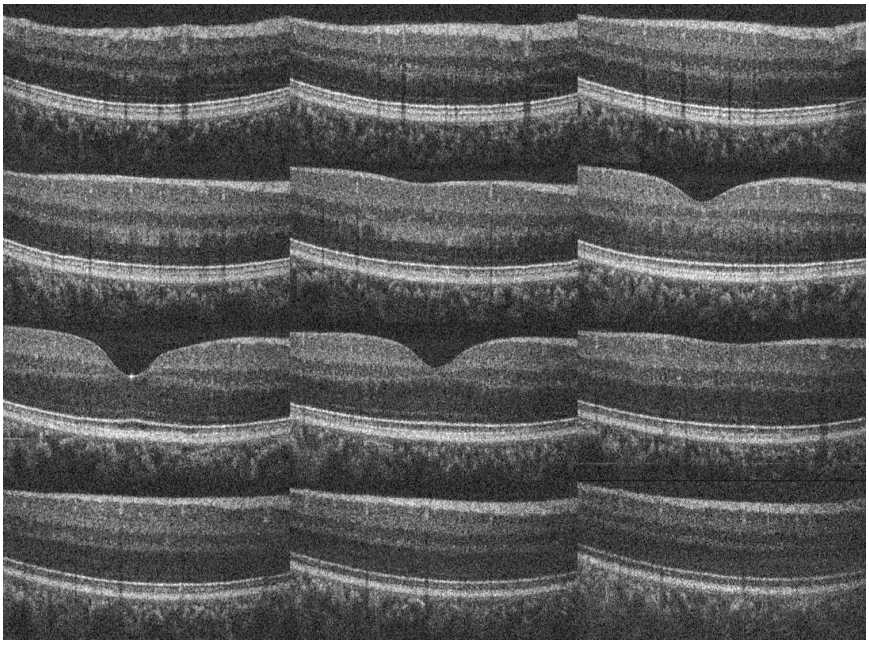

*Figure 6: Selected images from 100 B scans of the central macula in a control subject.*

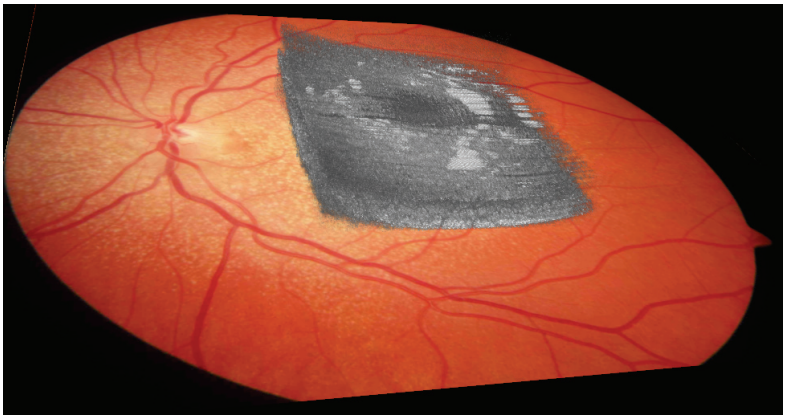

*Figure 7: Volumetric scan from 100 horizontal macular B scans overlaid on a fundus in a patient with EFEMP1 associated macular dystrophy.*

## 3. RESULTS OF PHENOTYPE CHARACTERIZATION

In the following, data of phenotype characterization in patients with different macular dystrophies are described. Genotype was available in all but two disease entities; age-related macular degeneration (AMD) and membrano-proliferative glomerulonephritis type II.
The initial projects in patients with AMD were focused to quantify retinal dysfunction, it's progression and relation to fundus morphology. Further investigations were performed in patients with macular dystrophies, which share the signs of 'retinal deposit disease': Stargardt Macular Dystrophy, autosomal dominant drusen, membrano-proliferative glomerulonephritis type II and autosomal recessive bestrophin retinopathy.
Patients with cone-rod dystrophies very often show an associated maculopathy. We therefore included patients with Bardet-Biedl-Syndrome in the imaging study.
X-linked retinoschisis, shows an early disease onset similar to Stargardt Macular Dystrophy but mostly without progression. It is considered as a vitreo-retinal dystrophy. There, we examined the retinal, specifically the photoreceptor changes with different ages.

### 3.1. Age-related Macular Degeneration (AMD)

An early sign of AMD are large drusen, which are highly predictive of late stage disease.[3, 32] Those deposits originating from photoreceptor outer segments are localized between the retinal pigment epithelium (RPE) and the inner collagenous zone of Bruch's membrane.[33] Histological data identified disrupted, rearranged and atrophic photoreceptors adjacent to and /over drusen.[33-35] We investigated the extent of retinal dysfunction measured by mfERG and its correlation to morphology. (Ref. 4, 5)[14, 15] 20 patients (31 eyes) ages 58 to 84 years with ≥5 large drusen were

included in the study. The change in response amplitude and implicit time in patients with large drusen who often retained visual acuity can be very small as illustrated in the example in Figure 8.

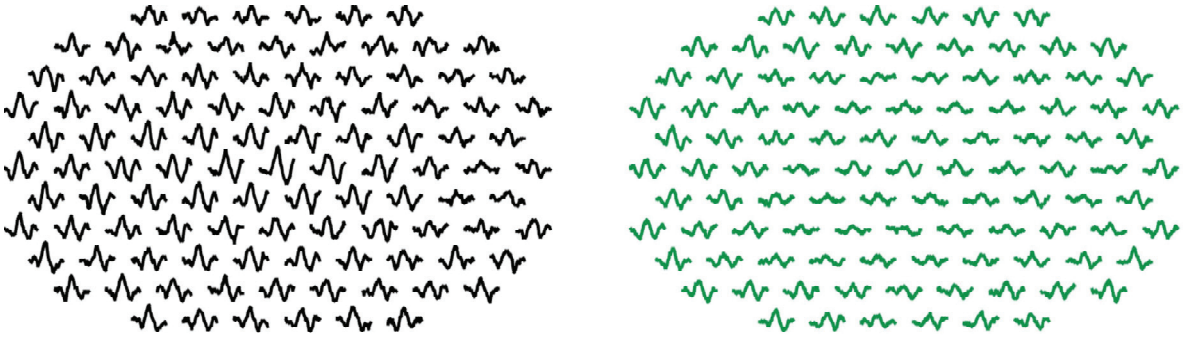

*Figure 8: Example of mfERG responses from a 68-year old patient with large drusen and visual acuity of 20/20 (green traces) compared with a 77 year old control subject (black traces).*

Here, we applied a localized response analysis of each of the 103 mfERG responses. Response averaging over a retinal area would have smoothed most of the abnormal responses due to the very distinct characteristics. Our data indicated that implicit times were more often abnormal than response amplitudes. Comparing different implicit times, N2 was more often delayed than N1 or P1.

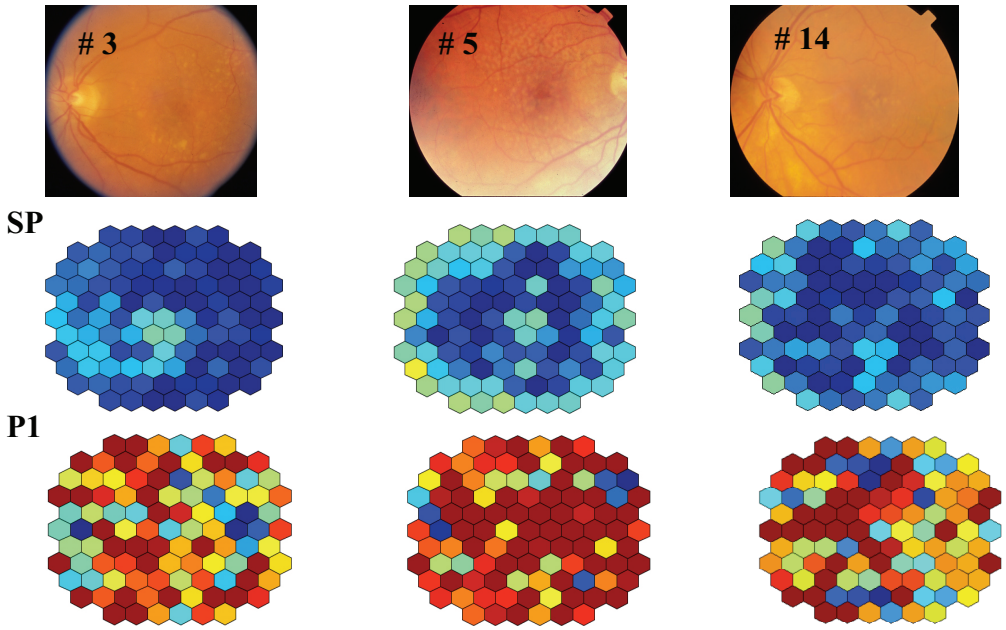


*Figure 9: Example of 3 eyes with retinal dysfunction not confined to the drusen area visible on the fundus photography (top row). Results of scalar products (SP) (middle row) and implicit time P1 (bottom row) illustrating extended retinal dysfunction. Color code: reduced SP < 2SD in dark blue, delayed P1 >2SD in red.*

Theses data suggest an earlier dysfunction in outer retinal cells other than photoreceptors. Functional data were correlated with the area of drusen measured on red-free fundus photography. Response abnormalities were found beyond morphological changes up to the entire retinal area tested. (examples in Fig. 9) We detected a significant correlation of drusen area and retinal responses in only a few patients. Those results indicate that patients with early stage AMD already have compromised function within the cone-driven pathways. The extent of dysfunction is not reflected by the ophthalmoscopically visible drusen but is more general over the retinal area.

We were then interested in the longitudinal disease course and re-tested most of the patients who participated initially after a follow up of 28 to 41 months. (Ref. 5)[15] MfERG results demonstrated a significant deterioration in all response components. (Fig. 10)

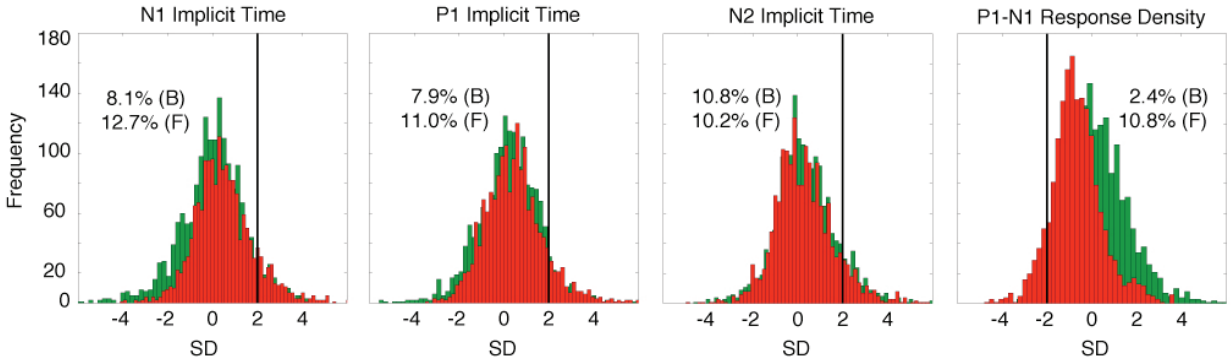


*Figure 10: Significant changes in implicit times N1, P1 and response density P1-N1at baseline (green histograms) and follow up (superimposed red histograms). Bold lines indicate the point of significant abnormal responses.*

The most dramatic response decline was evident in response density reduction, which was not confined to the central retina. Morphological analysis revealed drusen progression, unchanged drusen or drusen regression with an increase of RPE atrophy. Retinal function, in particular implicit times, behaved differently in those 3 groups. It appeared that drusen regression is associated with further implicit time delays. Thus, mfERG is a very useful tool quantifying retinal function in patients with early stage AMD. MfERG responses might be an important outcome measure in further studies and treatment trials. (Ref. 8) [36] Care, however, must be taken in data acquisition and data analysis. Comparison with age-matched control data, control for noise level[17] and a localized analysis approach are basis for successful interpretation.

### 3.2. Stargardt Macular Dystrophy

Stargardt Macular Dystrophy[1] (STGD1, OMIM248200) / Fundus flavimaculatus (FFM) is one of the most common hereditary macular dystrophy with a juvenile onset. It accounts for about 7% of all retinal dystrophies.[2] It often presents as a subacute but progressive decrease in visual acuity with a poor final visual outcome. One of the first clinical signs is a blunting of the foveal reflex. The macula can become progressively atrophic with a "beaten bronze" or "bull's eye" appearance. Classically, this is associated with a variable distribution of yellowish "pisciform" deep retinal flecks.[37-40] Central scotomas are the most common visual field abnormality.

STGD1 and FFM are different phenotypic severities caused by mutation in the *ABCA4* gene.[41] The same gene might play a role in the development of AMD, but this fact is discussed controversially.[42-44]

To determine the functional effect of *ABCA4* mutations in vivo, we investigated retinal function in 16 genotypic identified patients with STGD1/ FFM using psychophysical (visual acuity, color vision, two-color static perimetry) and electrophysiological measures (fullfield ERG, mfERG). (Ref. 1)[11] Perimetry data indicated dysfunction in the cone pathways in all but one patient tested. Fullfield ERG responses were within normal range in most of the patients. Abnormal mfERG responses, in contrast, reflected the predominantly affected central retina. Reduced response densities were found in all and delayed P1 implicit time in 80% of the patients. Even in early stages of the disease with still good visual acuity, we were able to reveal a significant response delay and/ or reduction using the mfERG test. (Fig. 11)

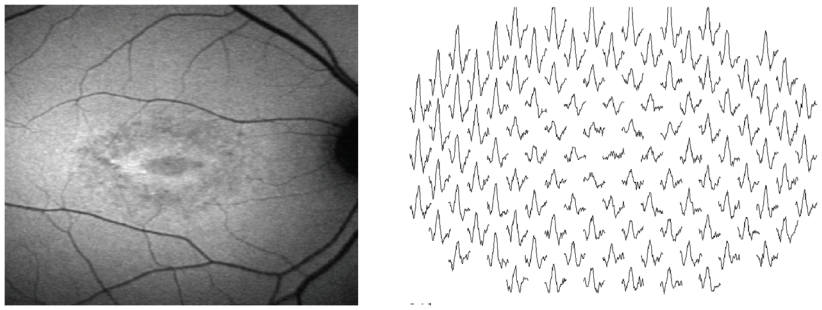

*Figure 11: Autofluorescence (AF) image of the right macula and mfERG response array elicited from the same fundus area in a patient with compound heterozygous ABCA4 mutation. Visual acuity: 20/40. Only central mfERG responses are reduced. Ring of increased AF surrounding a central reduced AF corresponding to increased lipofuscin and loss of RPE, respectively.*

Reduced mfERG responses identified the affected stage in the cone driven pathways, namely photoreceptor and bipolar cells. Thus, reduced sensitivity on two-color perimetry is caused by a dysfunction at an early stage of the cone pathways, within the outer retinal cells.
There was a significant association between disease duration and retinal function. Functional mfERG data together with psychophysical measures of cone and rod mediated function correlated with the present genotype. We found greater disease severity in patients with a homozygous mutation and compound heterozygous mutation with predicted loss of allelic function. Milder phenotype was evident in patients harboring less severe mutations with predicted partial protein activity.

The hallmark of STGD1 is the loss of foveal photoreceptors and the accumulation of lipofuscin granules in RPE cells as shown in histological sections by Birnbach et al. (Fig 12)[40]

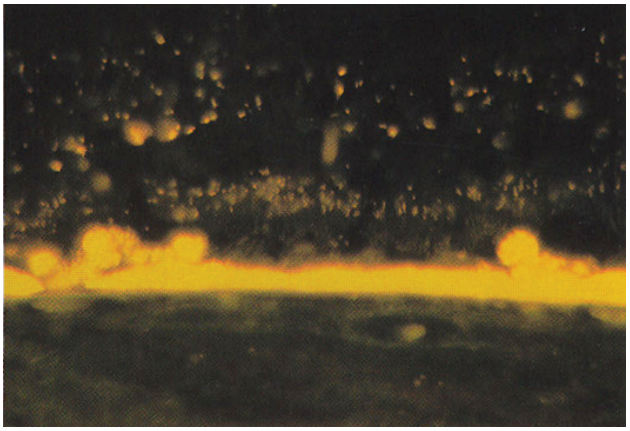

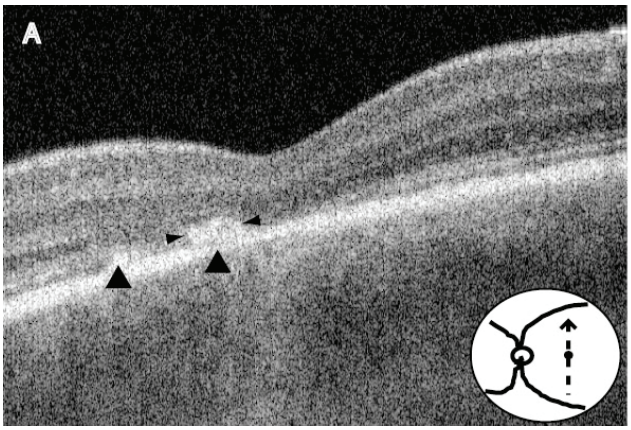


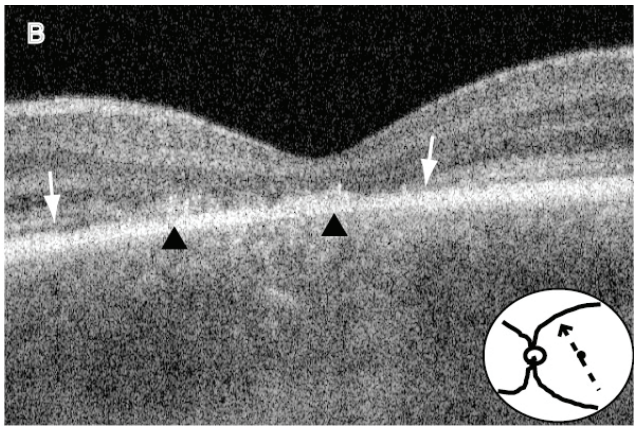


*Figure 12:Histological sections through the retina of a patient with STGD1 demonstrate lipofuscin accumulation within RPE cells. (left panel).[39] In vivo macular FD-OCT scans identified similar deposits in a patient with STGD1. (lower panel: A/B) Photoreceptor loss is visible in the central area (white arrows).*

In the pre-OCT era, no in-vivo method was available to visualize these changes within different retinal layers. Lipofuscin accumulation within the RPE cells can be shown indirectly by the

demonstration of increased autofluorescence.[45] (example in Fig. 11) The morphology of photoreceptor cells cannot be identified with this investigation. OCT, in particular high-resolution OCT techniques permit the identification of small retinal cell changes and the localization of retinal deposits. We showed for the first time retinal deposits of lipofuscin in a patient with STGD1. (Ref. 9)[46] (Fig. 12)

The comparison with Birnbach's[40] observations is striking. A similar shape and location of the deposits is shown in the retinal layer analysis. Outer retinal layers demonstrate changes sharply confined to the central macula: the outer nuclear layer is thinned or not identifiable, the inner and outer segment layers, connecting cilium and Verhoeff's membrane are not distinguishable. The lipofuscin deposits are within the RPE cell layer and 'replacing' outer retinal layers. Inner retinal layers are not affected in the patients who were tested. (unpublished data and [46]) (Fig. 12)
Based on these data it is now possible to correlate retinal function with detailed in-vivo acquired retinal abnormalities in STGD1.

### 3.3 Autosomal dominant drusen

Autosomal dominant drusen (ADD) (OMIM 126600) were originally described in two different geographical regions as Doyne Honeycomb Retinal Dystrophy (DHRD) in England[47] and Malattia Leventinese (MLVT) in Switzerland.[48] A single missense mutation Arg345Trp in the *EFEMP1* gene has been identified in both DHRD and MLVT.[49] Fundus changes show retinal deposits different in size and distribution compared with STGD1. Here, characteristic signs are early onset drusen at the posterior pole and peripapillar area with radial distribution and increasing confluence with age. Large cohort studies demonstrated phenotypic inter- and intrafamilar variability.[50, 51]
Vision function is better preserved than in STGD1. In a mild phenotype, diagnosis is made through a routine eye exam in patients without symptoms.
Multifocal ERG recording can reveal central cone-mediated dysfunction as shown in the case of a 30-year old patient with minimally reduced visual acuity (Snellen acuity 0.9) but obvious fundus changes. (Ref. 13)[52] Fullfield ERG data were within normal range. MfERG results revealed reduced and delayed responses within the central 20 degrees retinal eccentricity. (Fig. 13) With the well-preserved visual acuity one would not have expected such dramatic changes in the macular function detected by mfERG.

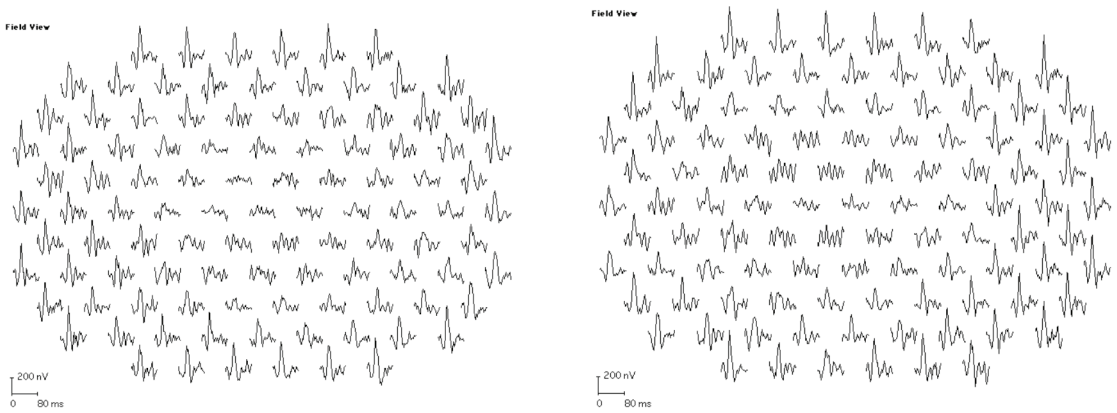


*Figure 13: MfERG trace arrays from a 30-year old patient with EFEMP1 associated macular dystrophy. Central responses are severely reduced. Some of the responses are not distinguishable from noise. Responses between 20° and 25° retinal eccentricity are within normal range.*

What are the associated retinal cell abnormalities and are those different from investigations in STGD1? Retinal layer analysis in *EFEMP1* associated macular dystrophy showed small to extensive deposits within the sub RPE cells. Bruchs membrane is separated from RPE cells. Outer retinal layers are elevated by the dense deposits and partially disrupted. Outer nuclear, inner and outer segment layers are thinner and sometimes not distinguishable. (Fig. 14)

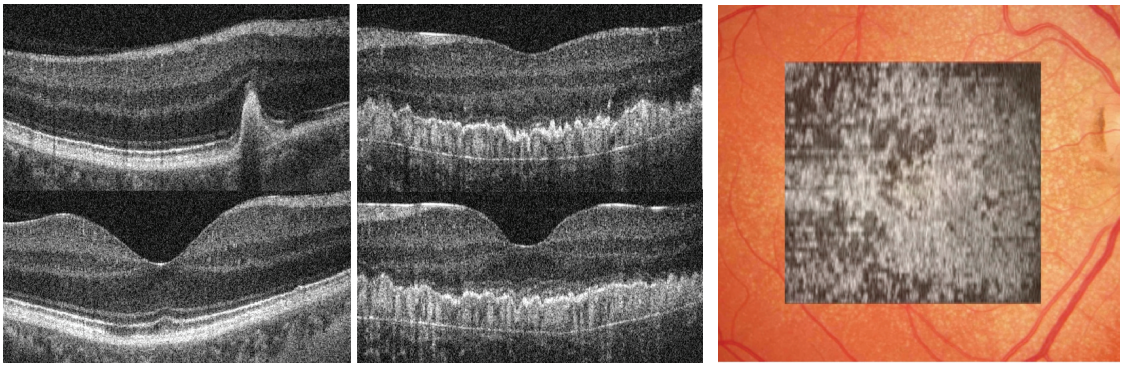

*Figure 14: Serial horizontal FD-OCT scans of 2 patients with EFEMP1 associated macular dystrophy demonstrate mild (left panel) to extensive (middle panel) deposits in the sub RPE space. Reconstructed C scan at the level of the photoreceptor inner/outer segment junction. (right panel)*

Inner retinal layers are undisturbed and intact. Volumetric scans as shown in Fig. 7 permit reconstruction of C scans of different retinal layers. Identification of deposits at the connecting cilium layer, the junction between inner and outer segments, was made possible through this C scan

and demonstrated the dimension of associated pathology. Photoreceptor disruption is confined to areas with sub RPE deposits. (Fig. 14)

### 3.3. Membrano-proliferative glomerulonephritis type II

Membrano-proliferative glomerulonephritis type II (MPGN type II or dense deposit disease[53]) is a rare disease affecting multiple systems such as kidneys (nephritic syndrome), heart (heart insufficiency), subcutaneous fat (lipodystrophy) and the retina (stable[54] to progressive[55] retinopathy).[56] MPGN type II is characterized by dense deposits within the glomerular basement membrane in the kindney and Bruch's membrane and choriocapillaris in the retina.[57, 58]
The retinal deposits are drusenoid and similar to autosomal dominant drusen.
We investigated the retinal localization and associated retinal layer disruption in different disease severities. (Ref. 12[59] and unpublished data)

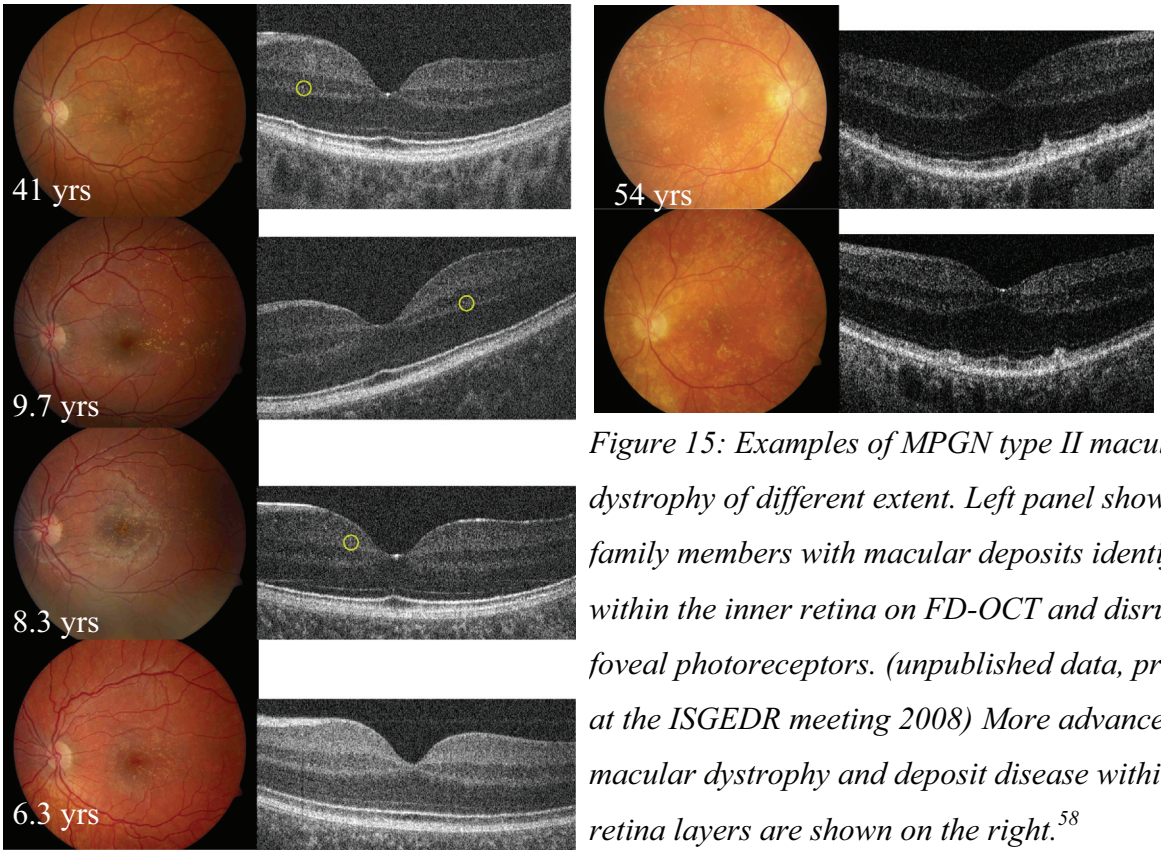


*Figure 15: Examples of MPGN type II macular dystrophy of different extent. Left panel shows 4 family members with macular deposits identified within the inner retina on FD-OCT and disrupted foveal photoreceptors. (unpublished data, presented at the ISGEDR meeting 2008) More advanced macular dystrophy and deposit disease within outer retina layers are shown on the right.*[58]

A family of three daughters and their mother showed distinct drusenoid deposits in the macular area of different distribution on a routine eye exam. Retinal function including visual acuity was normal. Kidney function was slightly abnormal suggesting MPGN type II. FD-OCT images revealed small

round deposits within the inner retinal layers. (Fig. 15) Of interest is the analysis of the foveal scans: disrupted Verhoeff's membrane was evident in all 4 patients. A more severe systemic and retinal phenotype was present in a 54 year old patient. In this case, we found dense deposits within the RPE/ Bruch's membrane protruding into outer retinal layers. Photoreceptor layers were disrupted not only in areas of retinal deposits but also in the foveal and macular areas without visible deposits. (Fig. 15)

### 3.4. Autosomal recessive bestrophin retinopathy

Best macular dystrophy[60] is an autosomal dominant macular dystrophy with variable phenotype and disease onset. Mutations in the *BEST1* gene are identified as disease causing.[61-63] The characteristic features are retinal deposits within the subretinal space, visible as 'egg yolk' lesions on ophthalmoscopy. Time-domain OCT localized retinal deposits within the outer retina or in the subretinal space.[64] A new type of macular dystrophy associated with biallelic mutations in the *BEST1* gene is referred as autosomal recessive bestrophin retinopathy (ARB).[65] Typical changes are multiple retinal deposits within the macula and possibly in the periphery. (Fig. 16) The deposits are

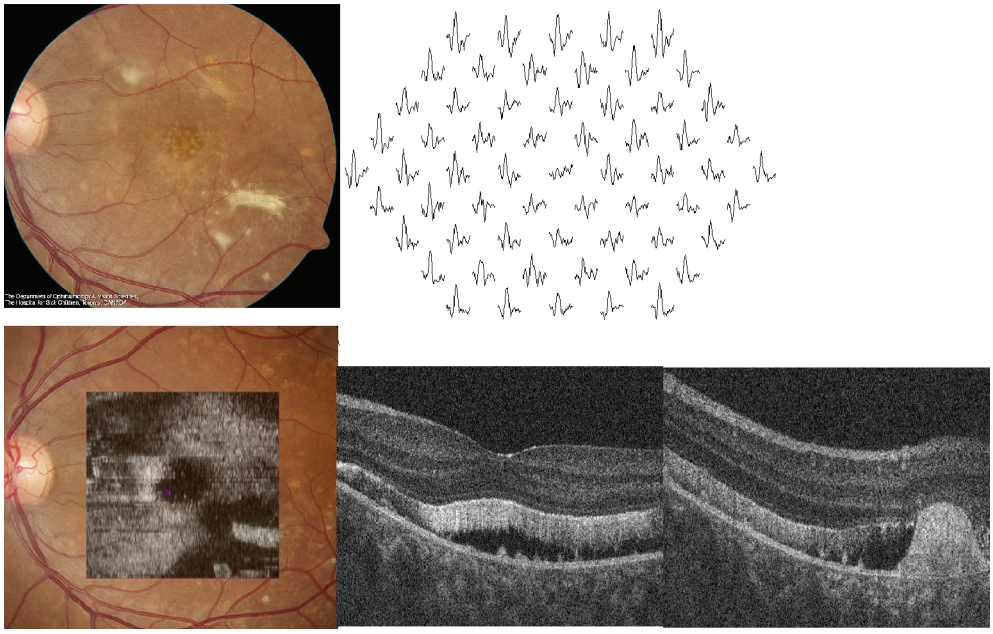

*Figure 16: Fundus images of the left eye shows multiple yellowish-white deposits within the macular area. Central mfERG responses are reduced and delayed (top row). OCT fundus at the level reconstructed at the level of the connecting cilium illustrated abnormal structure (bottom, left image). B scan OCT images reveal photoreceptor elongation and detachment and deposits within the RPE 'erupting' through outer retinal layers.*

different from autosomal dominant drusen, drusen in AMD or from the flecks seen in STGD1. In ARB, the deposits seem to be in deeper retinal layers and more indistinct. The RPE function is reduce as indicated by abnormal light rise and reduced Arden ration in electro-oculogram testing. We examined function and morphology in ARB to compare the changes with other retinal deposit diseases. (Ref. 15)[66] MfERG showed reduced and delayed responses within 10° retinal eccentricity. Normal mfERG responses between 10° to 25° were detected in areas with obvious fundus changes and retinal deposits. Normal visual acuity was found despite clear photoreceptor elongation in the foveal area. Deposits were very prominent reaching from the RPE into the subretinal space. (Fig. 16)

### 3.6. Maculopathy associated with retinopathy in Bardet-Biedl-Syndrome

Bardet-Biedl Syndrome (BBS) is a multi-systemic disorder with polydactyly, kidney abnormalities or dysfunction, retinopathy, obesity, learning disabilities or severe cognitive impairment.[67-70] Retinal dystrophy in patients with BBS includes a maculopathy in association with a generalized cone-rod dystrophy in most cases. The main research interest is the connecting cilium of the outer retina since BBS is thought to be a 'ciliopathy'.[71, 72] Functional data indicated a parallel but more severe disease progression in patients with mutations in *BBS10*.[73] No mfERG data are available in the patient group investigated with FD-OCT. Low visual acuity, nystagmus or attention or mental impairment did not allow successful mfERG recording.

We investigated retinal layer composition in patients with mutations in *BBS1* or *BBS10*, the most common disease causing mutations in BBS. (Ref. 11)[29] Results indicate predominant changes within outer retinal layers. Inner retinal layers showed normal configuration in all but one patient tested. This patient showed a severe retinopathy and maculopathy with reduced visual acuity to 0.05 (Snellen acuity). Outer retinal layers demonstrated preserved outer nuclear layers but thinned or indistinguishable outer and inner segment layers.

Connecting cilium was not identifiable in all patients scanned. Of interest are retinal deposits above or adjacent to Bruch's membrane. (examples in Fig. 17) Clinically, no retinal deposits such as seen in macular dystrophy described above were evident in patients with BBS. We presumed that the deposits are secondary to retinal degeneration as seen in patients with retinitis pigmentosa.[74] More severe retinal changes were found in patients with *BBS10* than *BBS1* mutation. A faster rate of progression might account for the retinal micro-structural advanced abnormalities in *BBS10* mutations.

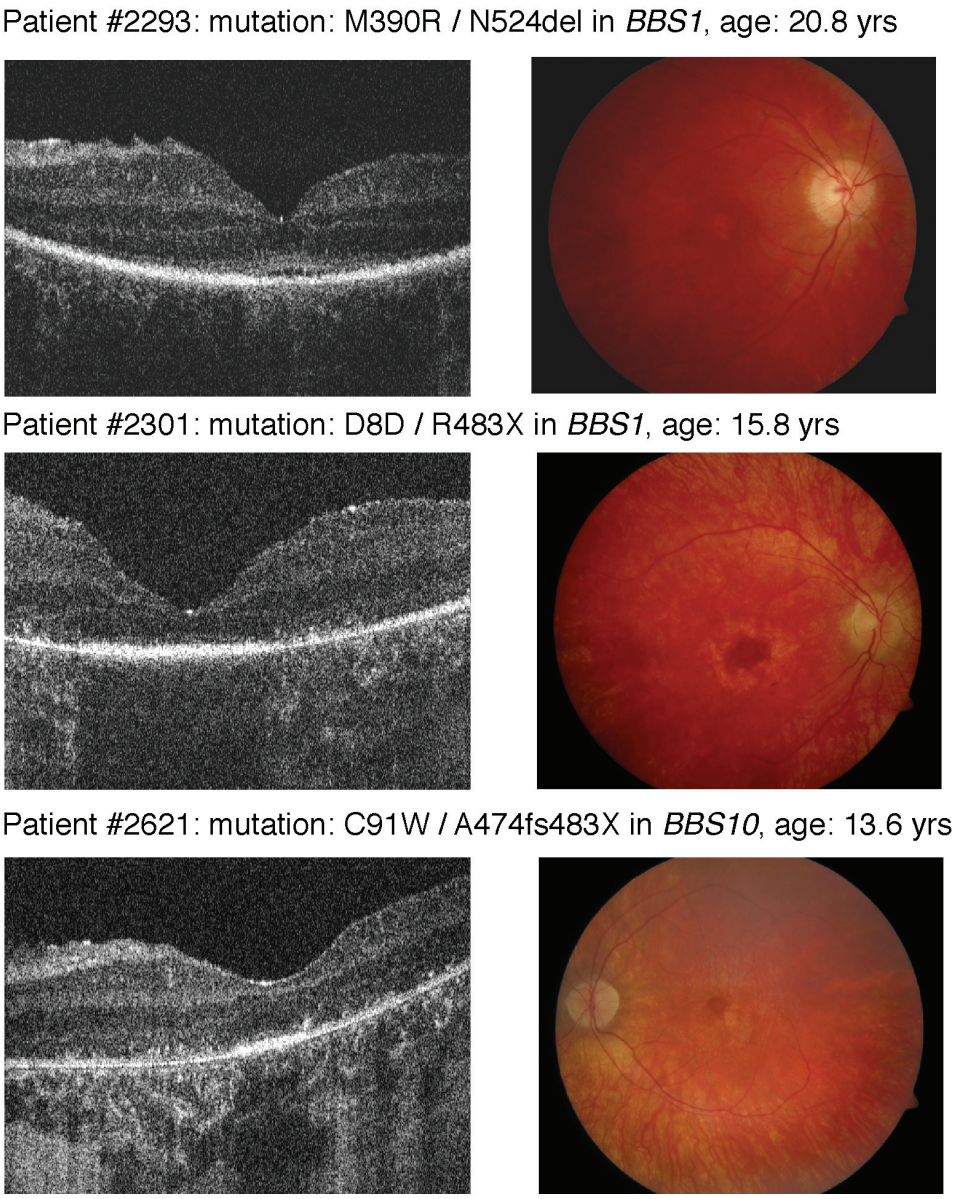


*Figure 17: Comparison of retinal morphology in patients with mutations in BBS1 and BBS10 revealed more advanced outer and inner segment atrophy, thinner RPE cell layer and more deposits above Bruch's membrane in patients with BBS10.*

### 3.5. X-linked Retinoschisis

X-linked Retinoschisis (XLRS)[75] caused by mutation in *XLRS1*[76] is a predominant macular vitreo-retinal dystrophy with splitting of the retina. (Fig. 18)

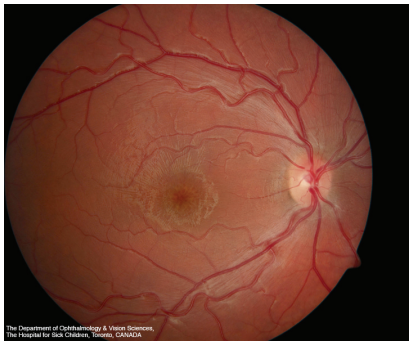

*Figure 18: Retinal splitting of the central macula is shown in a 6-year old boy with XLRS.*

Patients are of similar age or younger compared with patients with STGD1 when they report reduced vision or when it is discovered at a routine check up. Vision function can vary greatly from normal visual acuity to severely reduced.[77] It is considered as a stationary disease until a greater age. Then, atrophic changes are observed with associated reduction in vision. Retinal layer integrity and cell-cell interaction excluding photoreceptors are considered as the primary abnormal component in XLRS.

We examined patients of different ages with XLRS and identified mutation in *XLRS1* using FD-OCT to investigate the extent of photoreceptor involvement. (Ref. 10)[31] Our data showed that photoreceptors are indeed affected. (Fig. 19)

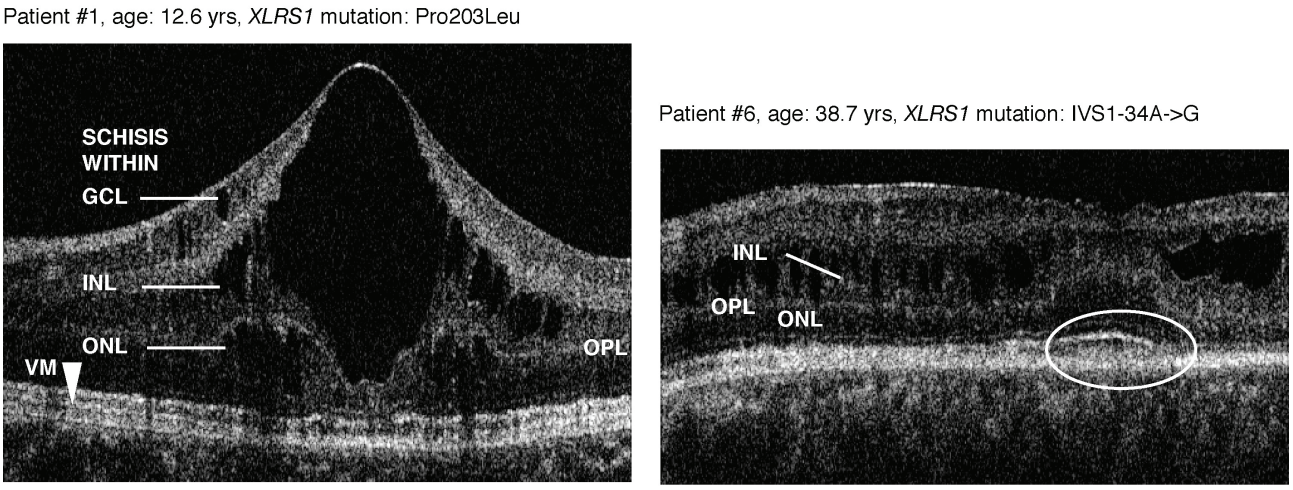


*Figure 19: Schisis localization is demonstrated in the foveal and extrafoveal region. Schisis extent is larger in younger patients and 'flattens' with age. Structural changes within photoreceptor layers are more progressed with greater age.*

Retinal schisis involved different retinal layers: inner plexiform to outer plexiform layers in the foveal region. Outer and inner nuclear and ganglion cell layers showed splitting in the extrafoveal area. Foveal outer and inner segment layers demonstrated irregularities and thinning with increasing

patients' age. Verhoeff's membrane, the interface between cone photoreceptor and RPE cells, was present in only the youngest patient tested and only in the extrafoveal area. There was no Verhoeff's membrane visible in all patients in the fovea, indicating a disruption of photoreceptor structure. Comparison of type of mutation or vision function with retinal morphology did not reveal a correlation. Higher age, in contrast, was associated with more progressed micro-structural retinal abnormalities.

## 4. CONCLUSION

MfERG and high resolution Fd-OCT techniques are powerful investigative tools to characterize phenotype variations in patients with various macular dystrophies. Both techniques provide results, which give together with other clinical parameter a comprehensive evaluation. Our results support that these methods are fundamental objective measures in patients with retinal dystrophies. Prerequisite for these investigations were extensive mfERG studies of aging effects and its origin.[12, 13]

Morphological and functional data are important to quantify underlying retinal dysfunction and structural changes to test for possible disease causing gene mutation. This is important particularly in less obvious phenotypes. For example, schisis identification by OCT together with fullfield ERG abnormalities will lead to investigation in the *XLRS1* gene. Extensive reduction in mfERG responses is seen more likely in patients STGD1 than in patients with autosomal dominant drusen. These data can guide molecular-genetic investigations.

We showed that the mfERG is a reliable objective measure of retinal function in longitudinal studies in patients with AMD.[15] Latency shifts in mfERG responses point to early disease abnormalities as shown in patients with large drusen in AMD.[14, 15] A careful achieved database together with a sophisticated data analysis allowed us to draw conclusions in respect to changes over time.

Morphology in retinal dystrophies was until recently only available in histological sections. Now, in-vivo OCT results can be compared with histological data. For example, patho-histological data support our findings of sub RPE deposits in autosomal dominant drusen.[78, 79] We showed that retinal deposits in patients with STGD1[46], autosomal dominant drusen[52], MPGN type II[80] or autosomal recessive bestrophin retinopathy[66] are of different retinal localization and extent. Investigation of the different photoreceptor layers in relation to retinal deposits is important for understanding disease mechanism. Are the deposits the primary site of pathology and associated

with inner and outer segment changes? For example, deposits in patients with BBS10 might be related to the fast time course of retinal degeneration in advanced disease stages with retinal re-organization.[29]

Functional and morphological results using mfERG and FD-OCT are important to verify disease hypothesis and animal models. Retinal structure changes in the *efemp1* retinal dystrophy mice model with deposits between the plasma and basement membrane of RPE cells parallel our in-vivo results in humans.[81, 82] Mice with *Bbs4* mutation showed similar changes compared with our FD-OCT human data with photoreceptor thinning and shortening of inner and outer segment layers.[83] Histopathological sections in patients with retinoschisis[84], murine models with $rs1^{-/y}$ and our results overlap in demonstrating focal and generalized photoreceptor abnormalities.

Visualization of distinct retinal changes will add to our understanding of gene function. Retinoschisin, the protein product of *XLRS1* expressed in photoreceptors and bipolar cells, is important to maintain retinal cell-cell interactions.[85] Our findings with retinal bridges between schitic areas are supportive of these findings.

Future studies will aim to quantify retinal changes early in disease process. The development of the flexible and modifiable FD-OCT unit with the hand-held scanner and possibly the application of adaptive optic system will permit retinal examination in patients any ages on cellular level.

## 5. REFERENCES

1. Stargardt K. Über die familiäre, progressive Degeneration in der Makulagegend des Auges. Albrecht von Graefes Archive Klin Exp Ophthal 1909;71:534-549.
2. Blacharski PA. Fundus flavimaculatus. In: Newsome DA, ed. Retinal dystrophies and degenerations. New York: Raven Press; 1988. p. 135-159.
3. Klein R, Klein BE, Linton KL. Prevalence of age-related maculopathy. The Beaver Dam Eye Study. Ophthalmology 1992;99:933-943.
4. Huang D, Swanson EA, Lin CP*, et al.* Optical coherence tomography. Science 1991;254:1178-1181.
5. Costa RA, Skaf M, Melo LA, Jr.*, et al.* Retinal assessment using optical coherence tomography. Prog Retin Eye Res 2006;25:325-353.
6. Podoleanu AG, Dobre GM, Cucu RG*, et al.* Combined multiplanar optical coherence tomography and confocal scanning ophthalmoscopy. J Biomed Opt 2004;9:86-93.
7. Marmor MF, Holder GE, Seeliger MW, Yamamoto S. Standard for clinical electroretinography (2004 update). Doc Ophthalmol 2004;108:107-114.
8. Sutter EE, Tran D. The field topography of ERG components in man--I. The photopic luminance response. Vision Res 1992;32:433-446.
9. Hood DC, Seiple W, Holopigian K, Greenstein V. A comparison of the components of the multifocal and full-field ERGs. Vis Neuroscience 1997;14:533-544.
10. Hood DC, Bach M, Brigell M*, et al.* ISCEV guidelines for clinical multifocal electroretinography (2007 edition). Doc Ophthalmol 2008;116:1-11.
11. Gerth C, Andrassi-Darida M, Bock M*, et al.* Phenotypes of 16 Stargardt macular dystrophy/fundus flavimaculatus patients with known ABCA4 mutations and evaluation of genotype-phenotype correlation. Graefes Arch Clin Exp Ophthalmol 2002;240:628-638.
12. Gerth C, Garcia SM, Ma L*, et al.* Multifocal electroretinogram: age-related changes for different luminance levels. Graefes Arch Clin Exp Ophthalmol 2002;240:202-208.
13. Gerth C, Sutter EE, Werner JS. mfERG response dynamics of the aging retina. Invest Ophthalmol Vis Sci 2003;44:4443-4450.
14. Gerth C, Hauser D, Delahunt PB*, et al.* Assessment of multifocal electroretinogram abnormalities and their relation to morphologic characteristics in patients with large drusen. Arch Ophthalmol 2003;121:1404-1414.
15. Gerth C, Delahunt PB, Alam S*, et al.* Cone-mediated multifocal electroretinogram in age-related macular degeneration: progression over a long-term follow-up. Arch Ophthalmol 2006;124:345-352.
16. Gerth C, Wright T, Heon E, Westall CA. Assessment of central retinal function in patients with advanced retinitis pigmentosa. Invest Ophthalmol Vis Sci 2007;48:1312-1318.
17. Wright T, Nilsson J, Gerth C, Westall C. A comparison of signal detection techniques in the multifocal electroretinogram. Doc Ophthalmol 2008;117:163-170.
18. Curcio CA, Millican CL, Allen KA, Kalina RE. Aging of the human photoreceptor mosaic. Visual Neurosci 1993;10:1081-1098.

19. Birch DG, Anderson JL. Standardized full-field electroretinography. Normal values and their variation with age. Arch Ophthalmol. 1992;110:1571-1576.

20. Weleber RG. The effect of age on human cone and rod Ganzfeld electroretinograms. Invest Ophthalmol Vis Sci 1981;20:392-399.

21. Wright CE, Williams DE, Drasdo N, Harding GFA. The influence of age on the electroretinogram and visual evoked potential. Doc Ophthalmol. 1985;59:365-384.

22. Schefrin BE, Werner JS, Plach M*, et al.* Sites of age-related sensitivity loss in a short-wave cone pathway. J Opt Soc Am A 1992;9:355-363.

23. Fortune B, Johnson CA. The decline of photopic multifocal electroretinogram responses with age is primarily due to pre-retinal optical factors. *J Opt Soc Am A* 2002;19:173-184.

24. Sutter EE. The interpretation of multifocal binary kernels. *Doc Ophthalmol.* 2000;100:49-75.

25. Shinomori K, Werner JS. Senescence of the temporal impulse response to a luminous pulse. Vision Res 2003;43:617-627.

26. Werner JS. Visual problems of the retina during ageing: Compensation mechanisms and colour constancy across the life span. *Prog. in Retinal and Eye Res.* 1996;15:621-645.

27. Wojtkowski M, Leitgeb R, Kowalczyk A*, et al.* In vivo human retinal imaging by Fourier domain optical coherence tomography. J Biomed Opt 2002;7:457-463.

28. Gerth C, Zawadzki RJ, Heon E, Werner JS. High-resolution retinal imaging in young children using a handheld scanner and Fourier-domain optical coherence tomography. J Aapos 2008.

29. Gerth C, Zawadzki RJ, Werner JS, Heon E. Retinal morphology in patients with BBS1 and BBS10 related Bardet-Biedl Syndrome evaluated by Fourier-domain optical coherence tomography. Vision Res 2008;48:392-399.

30. Sun W, Gerth C, Maeda A*, et al.* Novel RDH12 mutations associated with Leber congenital amaurosis and cone-rod dystrophy: Biochemical and clinical evaluations. Vision Res 2007:2055–2066.

31. Gerth C, Zawadzki RJ, Werner JS, Heon E. Retinal morphological changes of patients with X-linked retinoschisis evaluated by Fourier-domain optical coherence tomography. Arch Ophthalmol 2008;126:807-811.

32. Bressler SB, Maguire MG, Bressler NM, Fine SL. Relationship of drusen and abnormalities of the retinal pigment epithelium to the prognosis of neovascular macular degeneration. The Macular Photocoagulation Study Group. Arch Ophthalmol 1990;108:1442-1447.

33. Sarks SH, Sarks JP. Age-related maculopathy: Nonneovascular age-related macular degeneration and the evolution of geographic atrophy. In: Schachat AP, ed. Retina. St. Louis: Mosby-Year Book; 2001. p. 1064-1099.

34. Curcio CA, Medeiros NE, Millican CL. Photoreceptor loss in age-related macular degeneration. Invest Ophthalmol Vis Sci 1996;37:1236-1249.

35. Medeiros NE, Curcio CA. Preservation of ganglion cell layer neurons in age-related macular degeneration. Invest Ophthalmol Vis Sci 2001;42:795-803.

36. Gerth C. The role of the ERG in the diagnosis and treatment of Age-Related Macular Degeneration. Doc Ophthalmol 2008.

37. Steinmetz RL, Garner A, Maguire JI, Bird AC. Histopathology of incipient fundus flavimaculatus. Ophthalmology 1991;98:953-956.

38. Lopez PF, Maumenee IH, de la Cruz Z, Green WR. Autosomal-dominant fundus flavimaculatus. Clinicopathologic correlation. Ophthalmology 1990;97:798-809.

39. Klien BA, Krill AE. Fundus flavimaculatus. Clinical, functional and histopathologic observations. Am J Ophthalmol 1967;64:3-23.

40. Birnbach CD, Jarvelainen M, Possin DE, Milam AH. Histopathology and immunocytochemistry of the neurosensory retina in fundus flavimaculatus. Ophthalmology 1994;101:1211-1219.

41. Allikmets R, Singh N, Sun H*, et al.* A photoreceptor cell-specific ATP-binding transporter gene (ABCR) is mutated in recessive Stargardt macular dystrophy. Nat Genet 1997;15:236-246.

42. Allikmets R. Further evidence for an association of ABCR alleles with age-related macular degeneration. The International ABCR Screening Consortium. Am J Hum Genet 2000;67:487-491.

43. Dryja TP, Briggs CE, Berson EL, Rosenfeld PJ. ABCR-gene and age-related macular degeneration. Science 279: 1107. Science 1998;279:1107.

44. Rivera A, White K, Stohr H*, et al.* A comprehensive survey of sequence variation in the ABCA4 (ABCR) gene in stargardt disease and age-related macular degeneration. Am J Hum Genet 2000;67:800-813.

45. Delori FC, Staurenghi G, Arend O*, et al.* In vivo measurement of lipofuscin in Stargardt's disease--Fundus flavimaculatus. Invest Ophthalmol Vis Sci 1995;36:2327-2331.

46. Gerth C, Zawadzki RJ, Choi SS*, et al.* Visualization of lipofuscin accumulation in Stargardt macular dystrophy by high-resolution Fourier-domain optical coherence tomography. Arch Ophthalmol 2007;125:575.

47. Doyne RW. A peculiar condition of choroiditis occuring in several members of the same family. Trans Ophthalmol Soc UK 1899;19:71.

48. Vogt A. Die Ophthalmoskopie im rotfreien Licht. In: Graefe A, Saemisch T, eds. Handbuch der gesammten Augenheilkunde. Untersuchungsmethoden. Berlin, Leipzig: Verlag von Wilhelm Engelman; 1925. p. 1-118.

49. Stone EM, Lotery AJ, Munier FL*, et al.* A single EFEMP1 mutation associated with both Malattia Leventinese and Doyne honeycomb retinal dystrophy. Nat Genet 1999;22:199-202.

50. Edwards AO, Klein ML, Berselli CB*, et al.* Malattia leventinese: refinement of the genetic locus and phenotypic variability in autosomal dominant macular drusen. Am J Ophthalmol 1998;126:417-424.

51. Michaelides M, Jenkins SA, Brantley MA, Jr.*, et al.* Maculopathy due to the R345W substitution in fibulin-3: distinct clinical features, disease variability, and extent of retinal dysfunction. Invest Ophthalmol Vis Sci 2006;47:3085-3097.

52. Gerth C, Zawadzki RJ, Werner JS, Heon E. Retinal microstructure in patients with EFEMP1 retinal dystrophy evaluated by Fourier domain OCT. Eye 2008.

53. Alpers CE. The kidney. In: Kumar V, Abbas AK, Fausto N, eds. Pathological basis of disease. Philadelphia: Elsevier Saunders; 2005. p. 984-986.

54. D'Souza Y, Short CD, McLeod D, Bonshek RE. Long-term follow-up of drusen-like lesions in patients with type II mesangiocapillary glomerulonephritis. Br J Ophthalmol 2008;92:950-953.

55. Leys A, Proesmans W, Van Damme-Lombaerts R, Van Damme B. Specific eye fundus lesions in type II membranoproliferative glomerulonephritis. Pediatr Nephrol 1991;5:189-192.

56. Appel GB, Cook HT, Hageman G*, et al.* Membranoproliferative glomerulonephritis type II (dense deposit disease): an update. J Am Soc Nephrol 2005;16:1392-1403.

57. Duvall-Young J, MacDonald MK, McKechnie NM. Fundus changes in (type II) mesangiocapillary glomerulonephritis simulating drusen: a histopathological report. Br J Ophthalmol 1989;73:297-302.

58. Duvall-Young J, Short CD, Raines MF*, et al.* Fundus changes in mesangiocapillary glomerulonephritis type II: clinical and fluorescein angiographic findings. Br J Ophthalmol 1989;73:900-906.

59. Gerth C, Zawadzki RJ, Licht C*, et al.* A microstructural retinal analysis of membrano-proliferative glomerulonephritis type II. Br J Ophthalmol 2008:in press.

60. Best F. Über eine hereditäre Maculaaffection: Beiträge zur Vererbungslehre. Z Augenheikunde 1905:199-205.

61. Petrukhin K, Koisti MJ, Bakall B*, et al.* Identification of the gene responsible for Best macular dystrophy. Nat Genet 1998;19:241-247.

62. Stohr H, Marquardt A, Rivera A*, et al.* A gene map of the Best's vitelliform macular dystrophy region in chromosome 11q12-q13.1. Genome Res 1998;8:48-56.

63. Marquardt A, Stohr H, Passmore LA*, et al.* Mutations in a novel gene, VMD2, encoding a protein of unknown properties cause juvenile-onset vitelliform macular dystrophy (Best's disease). Hum Mol Genet 1998;7:1517-1525.

64. Spaide RF, Noble K, Morgan A, Freund KB. Vitelliform macular dystrophy. Ophthalmology 2006;113:1392-1400.

65. Burgess R, Millar ID, Leroy BP*, et al.* Biallelic mutation of BEST1 causes a distinct retinopathy in humans. Am J Hum Genet 2008;82:19-31.

66. Gerth C, Zawadzki RJ, Werner JS, Heon E. Detailed analysis of retinal function and morphology in a patient with autosomal recessive bestrophinopathy (ARB). Doc Ophthalmol 2008.

67. Bardet G. Sur un syndrome d'obésité congénitale avec polydactylie et réunite pigmentaire (contribution á l'etude des formes cliniques de l'obésite hypophysaire). Thése de Paris 1920;170:107.

68. Biedl A. Ein Geschwisterpaar mit adiposo-genitaler dystrophie. Dtsch Med Wschr 1922:1630.

69. Churchill DN, McManamon P, Hurley RM. Renal disease-a sixth cardinal feature of the Laurence-Moon-Biedl syndrome. Clin Nephrol 1981;16:151-154.

70. Schachat AP, Maumenee IH. Bardet-Biedl syndrome and related disorders. Arch Ophthalmol 1982;100:285-288.

71. Ansley SJ, Badano JL, Blacque OE*, et al.* Basal body dysfunction is a likely cause of pleiotropic Bardet-Biedl syndrome. Nature 2003;425:628-633.

72. Ross AJ, May-Simera H, Eichers ER*, et al.* Disruption of Bardet-Biedl syndrome ciliary proteins perturbs planar cell polarity in vertebrates. Nat Genet 2005;37:1135-1140.

73. Héon E, Gerth C, Elia Y, Munier F. Ocular phenotype comparison between patients with Bardet-Biedl Syndrome with identified *BBS1* and *BBS10* mutations. Invest Ophthalmol Vis Sci 2007:ARVO E-Abstract 3698.

74. Brosnahan DM, Kennedy SM, Converse CA*, et al.* Pathology of hereditary retinal degeneration associated with hypobetalipoproteinemia. Ophthalmology 1994;101:38-45.

75. Haas J. Ueber das Zusammenvorkommen von Veraenderungen der Retina und Chorioidea. Archive Augenheilkunde 1898;37:343-348.

76. Sauer CG, Gehrig A, Warneke-Wittstock R*, et al.* Positional cloning of the gene associated with X-linked juvenile retinoschisis. Nat Genet 1997;17:164-170.

77. Apushkin MA, Fishman GA, Rajagopalan AS. Fundus findings and longitudinal study of visual acuity loss in patients with X-linked retinoschisis. Retina 2005;25:612-618.

78. Collins ET. A pathological report upon a case of Doyne's chorioditis ("Honeycomb" or "family" choroiditis). The ophthalmoscope 1913:537-538.

79. Dusek J, Streicher T, Schmidt K. [Hereditary drusen of Bruch's membrane. II: Studies of semi-thin sections and electron microscopy results]. Klin Monatsbl Augenheilkd 1982;181:79-83.

80. Gerth C, Zawadzki RJ, Licht C*, et al.* A microstructural retinal analysis of membrano-proliferative glomerulonephritis type II. Br J Ophthalmol 2008;92:1150-1151.

81. Fu L, Garland D, Yang Z*, et al.* The R345W mutation in EFEMP1 is pathogenic and causes AMD-like deposits in mice. Hum Mol Genet 2007;16:2411-2422.

82. Marmorstein LY, McLaughlin PJ, Peachey NS*, et al.* Formation and progression of sub-retinal pigment epithelium deposits in Efemp1 mutation knock-in mice: a model for the early pathogenic course of macular degeneration. Hum Mol Genet 2007;16:2423-2432.

83. Eichers ER, Abd-El-Barr MM, Paylor R*, et al.* Phenotypic characterization of Bbs4 null mice reveals age-dependent penetrance and variable expressivity. Hum Genet 2006;120:211-226.

84. Condon GP, Brownstein S, Wang NS*, et al.* Congenital hereditary (juvenile X-linked) retinoschisis. Histopathologic and ultrastructural findings in three eyes. Arch Ophthalmol 1986;104:576-583.

85. Curat CA, Eck M, Dervillez X, Vogel WF. Mapping of epitopes in discoidin domain receptor 1 critical for collagen binding. J Biol Chem 2001;276:45952-45958.

## 6. LIST OF INCLUDED PUBLICATIONS

This work is based on the following published data and referred to it as a Reference (Ref.) throughout the text.

Multifocal Electroretinogram

1. *Gerth C*, Andrassi-Darida M, Bock M, Preising M, Weber B, Lorenz B
Phenotypes of 16 Stargardt/FFM disease patients with known *ABCA4* mutations and evaluations of genotype-phenotype correlation
Graefe's Clin Arch Exp Ophthalmol 2002; 240: 628-638

2. *Gerth C*, Garcia SM, Ma L, Keltner JL, Werner JS
Multifocal ERG: Age-related changes for different luminance levels
Graefe's Clin Arch Exp Ophthalmol 2002; 240: 202-208

3. *Gerth C*, Sutter EE, Werner JS
MfERG response dynamics of the aging retina
Invest Ophthalmol Vis Sci 2003; 44: 4443-4450

4. *Gerth C*, Hauser D, Delahunt PB, Morse LS, Werner JS
Assessment of multifocal electroretinogram abnormalities and their relation to morphologic characteristics in patients with large drusen
Arch Ophthalmol 2003; 121: 1404-1414

5. *Gerth C*, Delahunt PB, Alam S, Morse LS, Werner JS
Cone-mediated MfERG in AMD: progression over a long-term follow-up
Arch Ophthalmol, 2006, 124:345-352

6. *Gerth C*, Wright T, Heon E, Westall CA
Assessment of central retinal function in patients with advanced retinitis pigmentosa
Invest Ophthalmol Vis Sci, 2007, 48: 1312-1318

7. Wright T, Nielssen J, *Gerth C,* Westall C
A comparison of signal detection techniques in the multifocal electroretinogram
Doc Ophthalmol, 2008, 117:163-170

8. *Gerth C*
The role of the ERG in the diagnosis and treatment of Age Related Macular Degeneration.
Doc Ophthalmol, 2008, Jun 7 (Epub ahead of print)

High-resolution optical coherence tomography:

9. *Gerth C*, Zawadzki RJ, Choi SS, Keltner JL, Park SS, Werner JS
Visualization of Lipofuscin accumulation in Stargardt macular dystrophy by high-resolution Fourier-domain Optical Coherence Tomography
Arch Ophthalmol, 2007, 125: 575

10. *Gerth C*, Zawadzki RJ, Werner JSW, Heon E
Retinal morphology of patients with X-linked Retinoschisis evaluated by Fourier-Domain Optical Coherence Tomography
Arch Ophthalmol, 2008,126:807-811

11. *Gerth C*, Zawadzki RJ, Werner JSW, Heon E
Retinal morphology in patients with *BBS1* and *BBS10* related Bardet–Biedl Syndrome evaluated by Fourier-domain optical coherence tomography
Vis Res, 2008, 48: 392-399.

12. *Gerth C*, Zawadzki RJ, Licht C, Werner JSW, Heon E
A Microstructural retinal analysis of membrano-proliferative glomerulonephritis type II
BJO, 2008, 92: 1150-1160

13. *Gerth C*, Zawadzki RJ, Werner JSW, Heon E
Retinal Microstructure in patients with *EFEMP1* retinal dystrophy evaluated by Fourier-domain OCT.
Eye, 2008, Sep 12 (Epub ahead of print)

14. *Gerth C*, Zawadzki RJ, Werner JSW, Heon E
High-resolution retinal imaging of young children using a hand-held scanner and Fourier-domain OCT.
JAAPOS, 2008, Dec 31 (Epub ahead of print)

15. *Gerth C*, Zawadzki RJ, Werner JSW, Heon E
Detailed Analysis of Retinal function and morphology in a patient with autosomal recessive bestrophinopathy (ARB)
Doc Ophthalmol, 2008, Nov 5 (Epub ahead of print)

## 7. ACKNOWLEDGMENTS

I am grateful to my parents for their love and support through the years of study, research and work.

I would like to thank my mentors John S. Werner, PhD, for his research inspiration, intellectual stimulation and being a role model in research and Elise Héon, MD, for her ongoing research encouragement and for sharing her knowledge in the field of hereditary eye diseases.

The research would not have been successful without my colleagues, mentors and friends at UC Davis (Peter Delahunt, PhD, Susan Garcia, COT, Robert Zawadzki, PhD) and at the Hospital for Sick Children in Toronto (Rita Buffa, OA, Yesmino Elia, MSc, Lindsay Hampton, BPA, OA, Rita Nobile, MSc, Carole Panton, OC (C), Carol A. Westall, PhD, Tom Wright, BSc) for their great collaborations, support and just being there.

Studies were supported by:

| | |
|---|---|
| Germany: | DFG |
| | Pro Retina |
| Canada: | Sick Kids Research Institute's Restracomp Fund |
| | Foundation Finding Blindness |
| | Mira Godard Fund |
| USA: | NIH |
| | Research to Prevent Blindness Jules and Doris Stein Professorship (JSW) |
| | Albrecht Fund |